LA-UR- 02-6667

Approved for public release;
distribution is unlimited.

Title: ON THE DEGRADED EFFECTIVENESS OF DIFFUSION SYNTHETIC ACCELERATION FOR MULTIDIMENSIONAL SN CALCULATIONS IN THE PRESENCE OF MATERIAL DISCONTINUITIES

Author(s): James S. Warsa
Todd A. Wareing
Jim E. Morel

Submitted to: Proceedings of the 2003 Nuclear Mathematical and Computational Sciences Conference, Gatlinburg, TN, 6-11 April 2003

Los Alamos
NATIONAL LABORATORY

LA-UR-02-6667

Nuclear Mathematical and Computational Sciences: A Century in Review, A Century Anew
Gatlinburg, Tennessee, April 6-11, 2003, on CD-ROM, American Nuclear Society, LaGrange Park, IL (2003)

ON THE DEGRADED EFFECTIVENESS OF DIFFUSION SYNTHETIC ACCELERATION FOR MULTIDIMENSIONAL S_N CALCULATIONS IN THE PRESENCE OF MATERIAL DISCONTINUITIES

James S. Warsa, Todd A. Wareing, Jim E. Morel
Transport Methods Group
Los Alamos National Laboratory
Los Alamos, NM 87545-0001
warsa@lanl.gov, wareing@lanl.gov, jim@lanl.gov

ABSTRACT

We investigate the degradation in performance of diffusion synthetic acceleration (DSA) methods in problems with discontinuities in material properties. A loss in the effectiveness of DSA schemes has been observed before with other discretizations in two dimensions under certain conditions. We present more evidence in support of the conjecture that DSA effectiveness can degrade in multidimensional problems with discontinuities in total cross section, regardless of the particular physical configuration or spatial discretization. Through Fourier analysis and numerical experiments, we identify a set of representative problems for which established DSA schemes are ineffective, focusing on highly diffusive problems for which DSA is most needed. We consider a lumped, linear discontinuous spatial discretization of the S_N transport equation on three-dimensional, unstructured tetrahedral meshes and look at a fully consistent and a "partially consistent" DSA method for this discretization. We find that the effectiveness of both methods can be significantly degraded in the presence of material discontinuities. A Fourier analysis in the limit of decreasing cell optical thickness is shown that supports the view that the degraded effectiveness of a fully consistent DSA scheme simply reflects the failure of the spatially continuous DSA method in problems where material discontinuities are present.

Key Words: diffusion synthetic acceleration, discrete ordinates, deterministic transport methods, unstructured meshes

1 INTRODUCTION

The spatial discretization of the DSA diffusion equations has to be "consistent" with the S_N transport discretization to achieve the level of source iteration acceleration (effectiveness) that is predicted analytically for homogeneous problems [1–5]. Effectiveness alone (as measured by the spectral radius) is not enough to guage the potential performance of a DSA method. The overall efficiency of the method must also be considered. An efficient DSA scheme is one in which the spectral radius small enough *and* the cost of computing the DSA correction is small enough such that the transport solution is computed to a given tolerance with less overall computational effort than would otherwise be possible. In some cases, then, a DSA method that is not fully consistent might be more efficient despite being less effective.

Recently it has been shown that there are several different situations in which the effectiveness of a particular combination of S_N discretization and DSA scheme is reduced, whether consistent or not. One situation is when a method that is robust and effective on one kind of mesh is ineffective or unstable on another. A particular example is the M4S (modified four-step) DSA scheme, a method that is not fully consistent with the discontinuous FEM methods of the S_N discretizations for which it is intended [6].

Originally shown to be effective in one dimensional slab geometry and on two-dimensional rectangular Cartesian geometries. The M4S method was later found to be unstable on three-dimensional unstructured tetrahedral grids with linear elements [5]. Similarly, after the simplified WLA (S-WLA) method was shown to be unconditionally effective in one dimensional slab geometry [7], it was later shown that its effectiveness is reduced in multidimensional problems with optically thick cells and scattering ratios very close to 1.0 [5].

There is another situation in which DSA methods, even fully consistent ones, can lose their effectiveness: in multidimensional problems with discontinuities in material properties. Problems contain two or more materials with total cross sections, at least of one of which is diffusive. The problem may consist of relatively large regions of different materials sharing a common interface or it may be one in which the materials differ from cell-to-cell. Without loss of generality we will limit ourselves to problems with just two materials.

Such a situation was first identified by Azmy in two dimensional geometries [8, 9]. The problems contained alternating layers of two materials with different total cross sections, $\sigma_1 = \sigma$ and $\sigma_2 = 1/\sigma$, referred to as the Periodic Horizontal Interface (PHI) configuration. The analytical analysis in the limit of $\sigma \rightarrow 0$ showed that no diffusion discretizations, either cell- or edge-centered, could be unconditionally effective for the two dimensional discretizations on rectangular cells considered (nodal and weighted-diamond difference S_N methods in [8], and the weighted-diamond difference discretization of the even-parity S_N equations in [9]). Azmy also points out this loss of effectiveness is not seen for consistent methods in one dimension (when material discontinuities are present) the situation in which the notion of consistency was first demonstrated as a sufficient condition for the effectiveness of DSA [1, 2].

We would like to determine whether these observations depend on a particular spatial discretization or geometric configuration (like the PHI) and whether this is a general result for multidimensions that does not depend on the fact that the problem is spatially discretized.

Our approach is twofold. First, we examine the partially consistent S-WLA method and the fully consistent (FCDSA) method using a Fourier analysis of a linear discontinuous finite element (DFEM) spatial discretization three-dimensional tetrahedral meshes (see [5]). The spatial discretization and DSA methods are described in Section 2. Our investigation is similar to the original work in [8] and [9] except we use a three dimensional unstructured mesh, with a completely different geometric configuration and spatial discretization. Results of actual numerical computations for problems that correspond to the Fourier analysis are then shown that confirm the predicted behavior. Another set of numerical computations show that it is independent of the way in which the heterogeneities are introduced. The effectiveness of even the fully consistent DSA method degrades in the presence of material discontinuities, independent of the optical thickness. The partially consistent method is already loses its effectiveness to some extent when scattering ratios are large and cells are optically thick [5]; the presence of material discontinuities makes it worse. The degradation of both methods is most pronounced when (at least part of) the problem is diffusive. The Fourier analysis is presented in Section 3 and computational results are shown in Section 4. This addresses the first part of our question.

Second, based on the evidence from these results and the results in [8] and [9], we believe it is appropriate to conjecture that these observations stem from an inherent defect of DSA. That is, the loss in effectiveness of DSA in the presence of material discontinuities does not depend on the fact that we are working with a

spatially discretized form of the S_N equations and diffusion equation. Given that our our DFEM spatial discretization is convergent in the sense that it faithfully models the analytical S_N problem as the optical thickness of the spatially discretized heterogeneous problem approaches zero, a Fourier analysis of the fully consistent DSA scheme in this limit indicates the degradation in the effectiveness of DSA is an analytical result – a failure of the DSA method itself – in such problems. A study with increasingly discontinuous material properties in this limit supports our conjecture. The results are shown in Section 5.

2 DISCONTINUOUS FINITE ELEMENT DISCRETIZATION ON TETRAHEDRAL MESHES

2.1 Spatially Discretized S_N Equations

We will begin by presenting the linear discontinuous finite element method (DFEM) for the transport equation on tetrahedra. That is followed by a brief overview of the fully consistent and partially consistent DSA methods . Further details on the fully consistent scheme can be found in [5] and details of the partially consistent method can be found in [10].

The notation used here has the usual meaning [11] and we assume cgs units. Given an angular quadrature set with N specified nodes and weights $\{\hat{\Omega}_m, w_m\}$, a distributed source of particles $Q(\boldsymbol{r}, \hat{\Omega})$ and anisotropic scattering of order L, the monoenergetic, steady-state S_N transport equation in the three-dimensional domain $\boldsymbol{r} \in V$ with boundary $\boldsymbol{r}_s \in \partial V$, is

$$\hat{\Omega}_m \cdot \nabla \psi_m(\boldsymbol{r}) + \sigma_t(\boldsymbol{r})\psi_m(\boldsymbol{r}) = \sum_{l=0}^{L} \sigma_{s,l} \sum_{n=-l}^{l} Y_{ln}(\hat{\Omega}_m)\phi_l^n(\boldsymbol{r}) + Q(\boldsymbol{r}, \hat{\Omega}_m), \quad m = 1, \ldots, N. \tag{1a}$$

Here, $Y_{ln}(\hat{\Omega})$ are the normalized spherical harmonics functions and the scalar flux moments are

$$\phi_l^n(\boldsymbol{r}) = \sum_{m=1}^{N} w_m Y_{ln}(\hat{\Omega}_m)\psi_m(\boldsymbol{r}). \tag{1b}$$

For the remainder of the paper we will assume only isotropic scattering, for which we set $L = 0$ and $\sigma_{s,0} = \sigma_s$. The inhomogeneous source is also assumed to be isotropic, or $Q(\boldsymbol{r}, \hat{\Omega}) = Q_0(\boldsymbol{r})$.

The linear DFEM discretization is specified by the following variational formulation. It is written in source iteration form with iteration index ℓ. Given an angular flux expansion in terms of the four independent linear basis functions on a tetrahedral cell T_k,

$$\psi_{m,k} = \sum_{j=1}^{4} \psi_{m,j,k} L_j(\boldsymbol{r}), \tag{2a}$$

find the linear approximation for each angle $\hat{\Omega}_m$ that satisfies

$$\hat{\Omega}_m \cdot \left(\int_{\partial T_k} \hat{n}\, \psi_m^b\, u_j\, dS - \int_{T_k} \psi_{m,k}^{\ell+1} \nabla u_j\, dV \right) + \sigma_{tk} \int_{T_k} \psi_{m,k}^{\ell+1} u_j\, dV = \sigma_{sk} \sum_m w_m \int_{T_k} \psi_{m,k}^{\ell} u_j\, dV + \int_{T_k} Q_0 u_k\, dV \tag{2b}$$

for all linear trial functions $u_j, j = 1, \ldots, 4$ on cell T_k. The Galerkin approximation takes the trial functions to be the basis functions L_j, and the above expressions can be evaluated for each of these four

functions. This gives four equations for the four unknowns $\psi_{m,j,k}$ on the cell. Before carrying out the integrations in (2b), however, we first introduce the discontinuous approximation. Considering a cell k with face p whose outward normal is $\hat{n}_p$, the boundary terms ψ^b_m are defined as

$$\left(\hat{\Omega}_m \cdot \hat{n}_p\right)\psi^b_m = \begin{cases} \left(\hat{\Omega}_m \cdot \hat{n}_p\right)\psi^{\ell+1}_{m,i(p),k}, & \hat{\Omega}_m \cdot \hat{n}_j > 0, \quad \hat{n}_p \text{ in } V \\ \left(\hat{\Omega}_m \cdot \hat{n}_p\right)\psi^{\ell+1}_{m,i(p),l}, & \hat{\Omega}_m \cdot \hat{n}_p < 0, \quad \hat{n}_p \text{ in } V \backslash \partial V \\ \left(\hat{\Omega}_m \cdot \hat{n}_p\right)\Gamma(\hat{\Omega}_m), & \hat{\Omega}_m \cdot \hat{n}_p < 0, \quad \hat{n}_p \text{ on } \partial V \end{cases} \tag{2c}$$

where l is the cell that shares face p with cell k. The subscript $i(p)$ denotes three vertices i on a face p of a given cell. Simply put, if $\hat{n}_p$ is on the boundary of the problem domain V, then the boundary condition is used to define the incoming angular flux for the three points on a face; otherwise the internal or external values angular fluxes are used depending on the orientation of the cell face with respect to the quadrature direction. The discrete boundary conditions are vacuum, $\Gamma(\hat{\Omega}_m) = 0$, or $\Gamma(\hat{\Omega}_m) = \psi^{\ell+1}_{m',i(p),s}$ for reflective boundary conditions, where m' is determined by the relationship

$$\hat{\Omega}_{m'} = \hat{\Omega}_m - 2\,\hat{n}\left(\hat{\Omega}_m \cdot \hat{n}\right), \tag{2d}$$

for $\hat{\Omega}_m$ and $\hat{n} = \hat{n}_p$. In our application, reflection is implemented only for boundary faces aligned parallel to the x, y or z coordinate axes so that the standard quadrature sets we use contain the reflected angles $\hat{\Omega}_{m'}$ that satisfy this relationship.

The integrals in (2) are evaluated, either analytically or by quadrature approximation, for every cell in the mesh. The angular flux, $\psi_{m,i,k}$, can then be computed for all vertices $j = 1, 4$ of every cell k, one cell at a time over the entire mesh in a predetermined order for every quadrature angle $\hat{\Omega}_m$. Note that we use a fully lumped version of (2). Describing it goes beyond the scope of this work, but suffice it to say that this lumping preserves the diffusion limit in thick, diffusive regimes (see [12]).

2.2 Source Iteration and DSA

The discretized S_N equations can be written in operator notation as

$$\boldsymbol{L}\psi = \boldsymbol{MSD}\psi + q. \tag{3}$$

The meanings of these operators can be easily deduced by comparison with (1a) and 2). With an an N-point quadrature and N_C spatial cells in the problem ψ be the vector of angular fluxes for every angle and every vertex (four of them) in each cell, so that ψ is of length $n = 4N_C \cdot N$. The vector q is an inhomogeneous source vector also of length n. The vector ϕ contains the scalar fluxes at the four vertices of each cell so that is is of length $4N_C$.

Rearranging (3) and introducing an iteration index ℓ, we get traditional source (or Richardson) iteration:

$$\psi^{\ell+1} = \boldsymbol{L}^{-1}\boldsymbol{MS}\phi^{\ell} + \boldsymbol{L}^{-1}q \tag{4a}$$

$$\phi^{\ell+1} = \boldsymbol{D}\psi^{\ell+1}. \tag{4b}$$

As written, the iteration works with the scalar flux as the primary quantity while the angular flux acts as an auxiliary quantity. This saves memory for problems with low degrees of scattering anisotropy and/or

multigroup energy dependence with many groups. However, working with the scalar flux means that reflective boundary conditions have to be treated specially in order to retain the angular information on reflective boundary faces. We will ignore this issue for our purposes here, with no loss of generality. The basic equations still hold, just the definition of the operators in (4) change slightly.

Equations (4) can be collapsed into a single iteration for the scalar flux, or

$$\phi^{\ell+1} = \boldsymbol{T}\boldsymbol{S}\phi^{\ell} + b \tag{5}$$

where $\boldsymbol{T} = \boldsymbol{D}\boldsymbol{L}^{-1}\boldsymbol{M}$ and $b = \boldsymbol{T}q$. It is easy to see that the convergence of source iteration, also known as Richardson iteration, is governed by the spectral radius of the operator $\boldsymbol{T}\boldsymbol{S}$. The spectral radius is bounded above by the maximum scattering ratio $c = \sigma_{sk}/\sigma_{tk}$ on the mesh (we assume $c \leq 1$) [2]. This implies that for highly scattering, diffusive problems with $c \approx 1$ this iteration is expected to converge slowly, making a solution costly or even impractical. Diffusion synthetic acceleration modifies the source iteration algorithm by computing a correction to the scalar flux, where the diffusion equation is used as an approximation to the transport operator [2, 13–15]. For homogeneous problems it can be shown that DSA reduces the spectral radius to approximately $0.225c$ (without angular discretization) [2, 5].

We will briefly review the DSA method now to put it in context. If ϕ is the exact solution to (5) then the error $f^{\ell+1} = (\phi - \phi^{\ell+1})$ satisfies

$$(\boldsymbol{I} - \boldsymbol{T}\boldsymbol{S})f^{\ell+1} = \boldsymbol{T}\boldsymbol{S}r^{\ell}, \tag{6}$$

where $r^{\ell} = (\phi^{\ell+1} - \phi^{\ell})$ is the residual. Equation (6) suggests that we can use an approximation to the operator $(\boldsymbol{I} - \boldsymbol{T}\boldsymbol{S})^{-1}\boldsymbol{T}\boldsymbol{S}$ to estimate the error and correct the current iterate. This will lead to a more efficient iteration if the approximate operator is relatively easy to setup and invert and if the approximate operator adequately reduces the spectral radius.

In the case of DSA, the approximate operator involves the diffusion operator, $\boldsymbol{C}$. This is an appropriate choice because the diffusion equation is the asymptotic limit of the transport operator in highly diffusive regimes [16, 17], just the situation for which we need acceleration. The diffusion operator is effective because it represents well the errors that are poorly attenuated by source iteration. Whether the diffusion operator can be inverted easily and lead to a more efficient algorithm depends on the spatial discretization of both the transport equation and the diffusion equation. Introducing an intermediate correction step in the source iteration algorithm, the DSA algorithm is

$$\phi^{\ell+1/2} = \boldsymbol{T}\phi^{\ell} + b \tag{7a}$$

$$f^{\ell+1/2} = \boldsymbol{C}^{-1}\boldsymbol{S}\left(\phi^{\ell+1/2} - \phi^{\ell}\right) \tag{7b}$$

$$\phi^{\ell+1} = \phi^{\ell+1/2} + f^{\ell+1/2}. \tag{7c}$$

The operator $\boldsymbol{C}^{-1}$ represents the "action" of the diffusion operator on the quantity $\boldsymbol{S}\left(\phi^{\ell+1/2} - \phi^{\ell}\right)$. Analytically the operator $\boldsymbol{C}$ is the diffusion equation and $\boldsymbol{C}^{-1}$ is simply its inverse. For our DFEM spatial discretization, however, $\boldsymbol{C}^{-1}$ represents more than just the inverse of spatially discretized diffusion equation. Certain projection and interpolation operations may be needed as well. The properties of the collection of computations represented by the $\boldsymbol{C}^{-1}$ operator determines how effective, efficient and robust the overall DSA algorithm will be.

We will consider two different definitions for the operator $\boldsymbol{C}^{-1}$. One is the fully consistent method based on a linear discontinuous discretization of the P_1 equations that has been described in [5]. Solution of the

corresponding large, sparse, linear system gives the necessary discontinuous scalar flux corrections. Unfortunately, this linear system (which can be written either in symmetric, indefinite form or nonsymmetric, positive definite form) was very difficult to solve, despite having developed an effective preconditioner. As a result, the overall cost of the transport solution accelerated with this DSA scheme did not always improve.

The other DSA method we consider is a partially consistent scheme, the S-WLA method. The basic theme of the method is quite simple. A finite element projection of the residual in the discontinuous scalar fluxes is computed. The projected residual is then used as the source term for a linear continuous finite element discretization of the diffusion equation. This discretization for the scalar fluxes is centered on the mesh vertices, which in part contributes to its efficiency on tetrahedral meshes for which there are typically 4-5 more cells than vertices. Furthermore, the linear system is symmetric and positive definite so conjugate gradients can be be used to efficiently solve the linear system. From this solution on the vertices, a correction to the discontinuous scalar fluxes is computed using the approach described in [10] for general meshes and arbitrary geometry.

Both methods will be examined in the following sections through Fourier analysis and numerical examples. A fully consistent scheme should be the best possible method while a partially consistent or inconsistent method is expected to be somewhat less effective. We find, however, that neither of them is unconditionally effective in problems with discontinuities in material properties.

3 FOURIER ANALYSIS

In this section we present a Fourier analysis of source iteration convergence for both the FCDSA and S-WLA methods with the linear DFEM discretization on tetrahedral meshes.

The Fourier analysis begins by dividing a three-dimensional box, or basic element, into six tetrahedra of equal volume. The orientation of the tetrahedra cell edges with this subdivision allows us to "tile" a volume with these basic elements. The box is of dimension $(\Delta x \times \Delta y \times \Delta z)$ as shown in Fig. 1. We can analyze the effects of material discontinuities for heterogeneous problems by assigning total cross sections $\sigma_{t,1}$ and $\sigma_{t,2}$ to the two halves of the basic element as indicated, each half consisting of three tetrahedra. The Fourier analysis procedure is implemented via the symbolic algebra program MAPLE. The details are described in [5] and modified to account for two materials. This basic element is assumed to repeat periodically in three dimensions through a Fourier ansatz of both the discontinuous and the continuous, vertex-centered unknowns. The transport and DSA equations are written by MAPLE in terms of the Fourier ansatz. The resulting 24×24 matrix is evaluated as a function of the element dimensions Δx, Δy, and Δz, the material properties c, $\sigma_{t,1}$ and $\sigma_{t,2}$, and the Fourier wave vector $[\lambda_x, \lambda_y, \lambda_z] \in [0, 2\pi] \times [0, 2\pi] \times [0, 2\pi]$ given a particular quadrature set. The space of wave numbers is searched with a simplex optimization algorithm to compute the maximum eigenvalue, the spectral radius, for a set of dimensions and material properties.

The spectral radius predicted by Fourier analysis was calculated over a range of cross sections, scattering ratios, and cell shapes, attempting to account for the range of problems we expect to encounter in our applications. An S_4 triangular Chebyshev-Legendre quadrature is used for which the analytical DSA spectral radius in homogeneous problems is $0.2543c$. The dimensions of the box are fixed, $\Delta x, \Delta z, \Delta y = 1.0$. The results for the S-WLA method are shown in Fig. 2 and results for the FCDSA method are shown in Fig. 3 for the scattering ratios $c = 0.9999, 0.999, 0.99$, and 0.9, Each plot has eleven

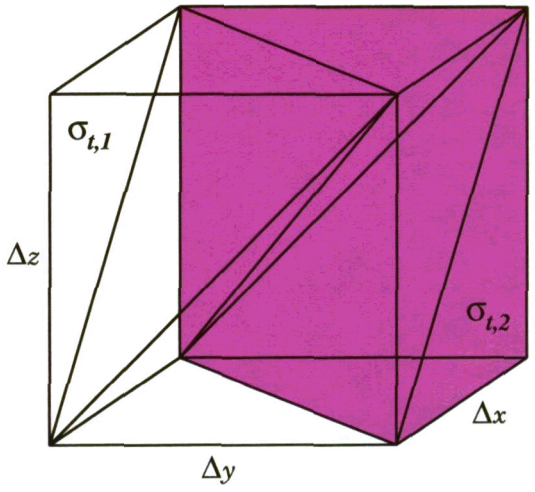

Figure 1. The basic element divided into 6 tetrahedra of equal volume. The two regions, each of which consists of three tetrahedra, contain materials with total cross sections $\sigma_{t,1}$ and $\sigma_{t,2}$.

curves on it that show the spectral radius as $\sigma_{t,2}$ varies over about six orders of magnitude for a range of eleven fixed values of $\sigma_{t,1}$, which vary of the same range as $\sigma_{t,2}$. The curves for $\sigma_{t,1} < 1$ have their minimum close to the analytical value. There is a strong dependence on the scattering ratio in the problem as $c \rightarrow 1$ that is more pronounced for the partially consistent DSA scheme in the optically thick limit. When the one or both of the cross sections is very large, FCDSA is much more effective than the S-WLA method and it does even better when both cross sections are large. However, when the scattering gets closer to one, there is always some loss in effectivess. The most important observation to note is that neither method can not be reliably depended upon to reduce the spectral radius as $c \rightarrow 1$. It is now clear that consistency alone does not ensure that a DSA method will be unconditionally effective in all problems.

Note that Fourier analysis was repeated with a basic element divided into 24 tetrahedra instead of six. The results agreed to at least three digits implying that analysis with six tetrahedra provides adequate spatial resolution.

4 NUMERICAL RESULTS

In this section we present the results of numerical computations with the unstructured tetrahedral mesh transport code AttilaV2. They are intended to verify the results of the Fourier analysis.

The first set of results is for a mesh consisting of a $(6 \times 6 \times 6)$ "grid" of cubes, each $(1.0$ cm on a side. Every cube is divided into six tetrahedra, three of which have total cross section $\sigma_{t,1}$ and three of which have total cross section $\sigma_{t,2}$, just like the basic element used in the Fourier analysis. The scattering ratio is fixed at $c = 0.999$ and vacuum boundary conditions are specified for all six faces of the problem.

The results of the Fourier analysis will be compared to the spectral radius measurements made with AttilaV2. Starting with a random scalar flux distributed over the mesh, the spectral radius is estimated by

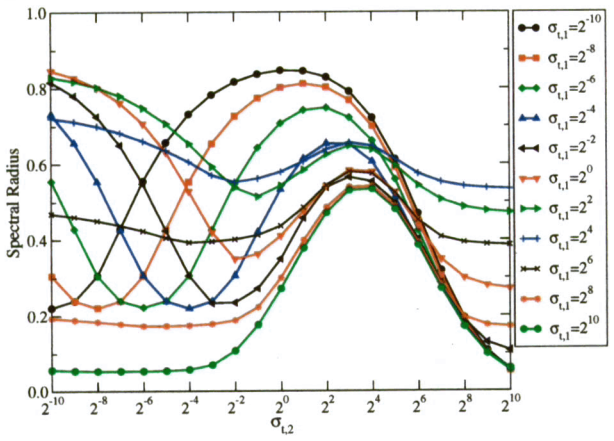

2(a) $c = 0.9$

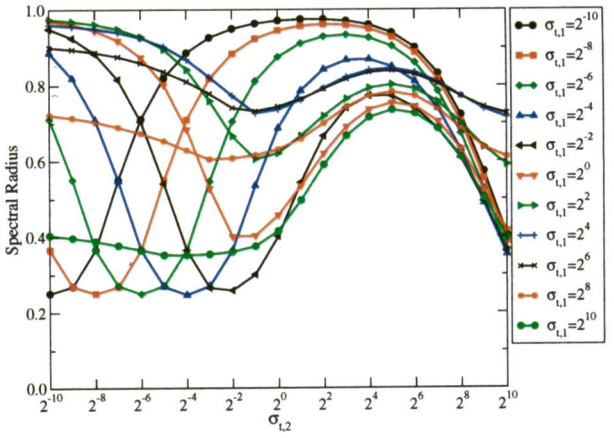

2(b) $c = 0.99$

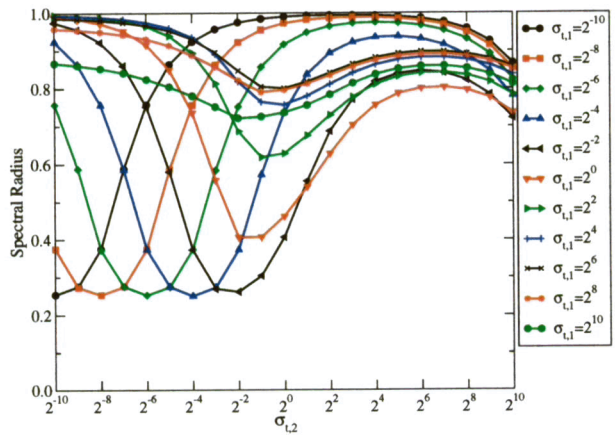

2(c) $c = 0.999$

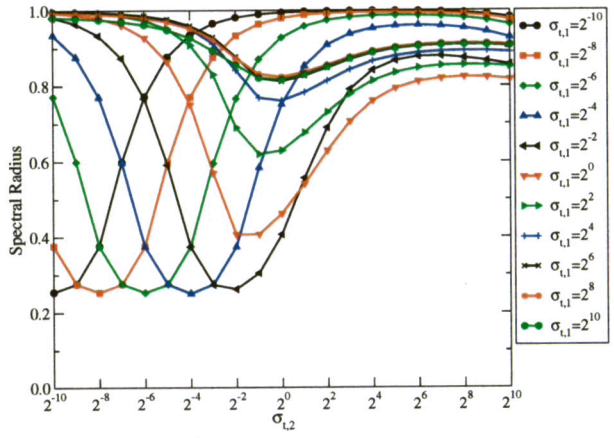

2(d) $c = 0.9999$

Figure 2. Fourier analysis for the S-WLA DSA method in heterogeneous problems containing two materials with total cross sections $\sigma_{t,1}$ and $\sigma_{t,2}$.

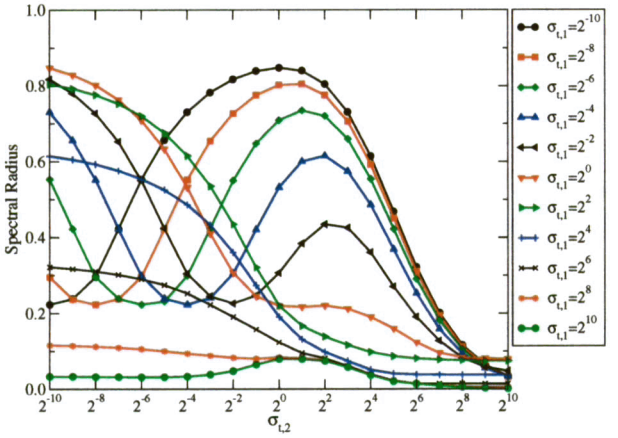

3(a) $c = 0.9$

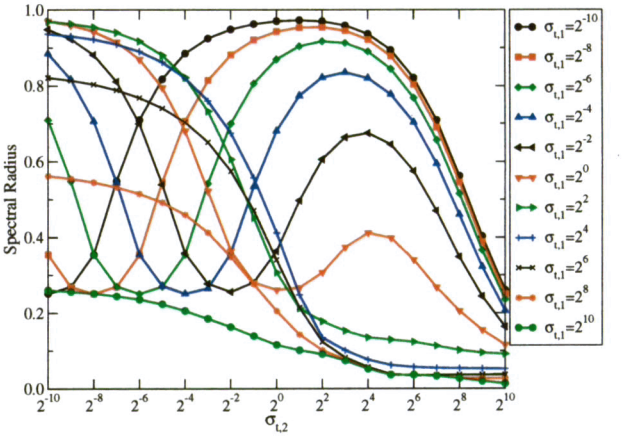

3(b) $c = 0.99$

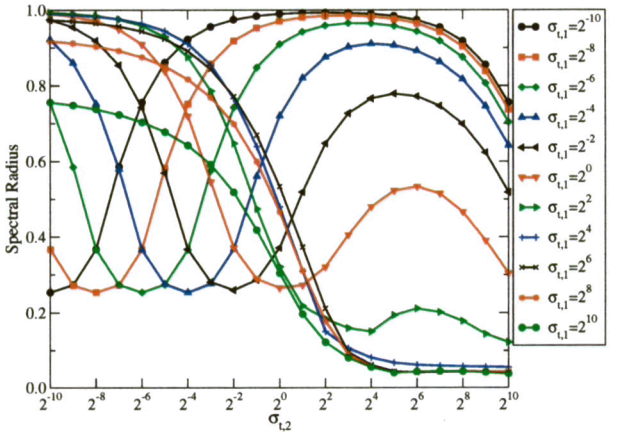

3(c) $c = 0.999$

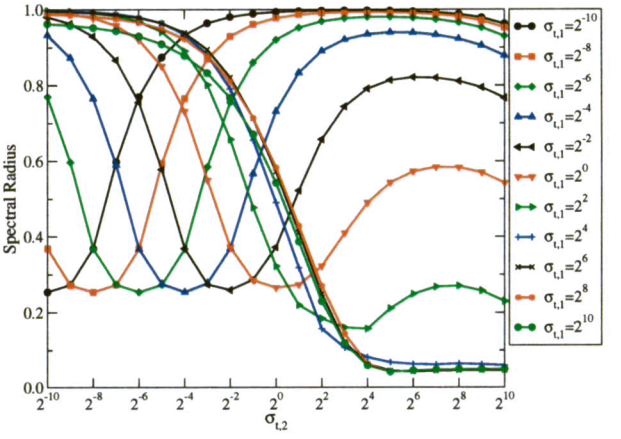

3(d) $c = 0.9999$

Figure 3. Fourier analysis for the Fully Consistent DSA method in heterogeneous problems containing two materials with total cross sections $\sigma_{t,1}$ and $\sigma_{t,2}$.

taking the ratio of the residual at two successive iterations, that is,

$$\rho \approx \frac{\|\phi^{\ell+1} - \phi^{\ell}\|_2}{\|\phi^{\ell} - \phi^{\ell-1}\|_2},$$

and renormalizing the scalar flux to $\|\phi^{l+1}\|_2$ after each iteration ℓ. The value reported after 100 iterations is shown in the figures, which we observed was more than enough to reach a value that was not changing in the fourth digit. The stopping tolerance used in the inner DSA iterations was fixed at 10^{-6}. Fig. 4 shows the spectral radius measurements for the S-WLA method for fixed $\sigma_{t,1} = 2^{-2}, 2^4, 2^{10}$ as $\sigma_{t,2}$ is varied compared to the Fourier analysis of the previous section. Fig. 5 shows the same set of measurements made using the FCDSA method. The measured values agree very well with the Fourier analysis. However, when the cross sections are small the problem domain is optically thin and leakage from the problem reduces the spectral radius relative to the Fourier analysis, which implicitly assumes an infinite medium. These results confirm that the loss in the effectiveness of DSA that was predicted by the Fourier analysis occurs in actual computations.

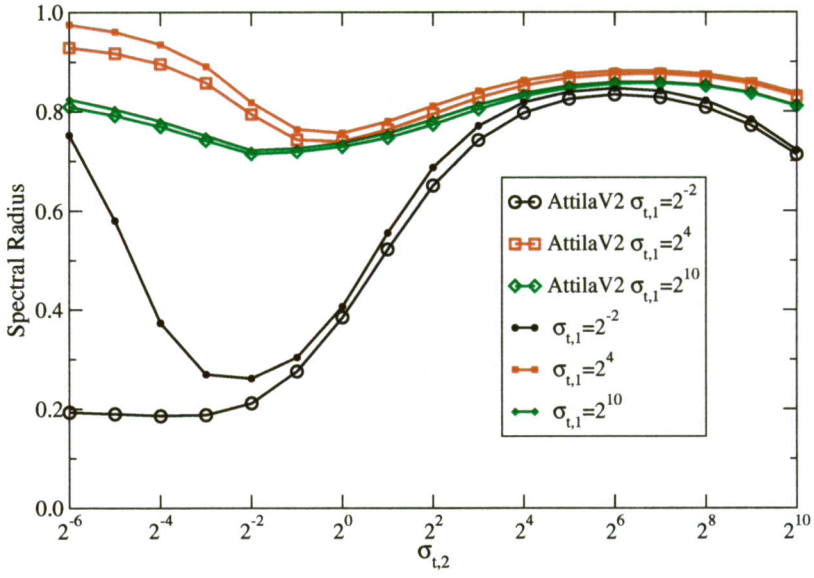

Figure 4. The spectral radius for the S-WLA method with $c = 0.999$ measured with the AttilaV2 code and compared to selected Fourier analysis results from the previous section.

The next set of results is ifor a more realistic problem. The idea is to show that there is nothing special about the cell-to-cell material discontinuities modelled by the Fourier analysis. The mesh consists of two regions, a box with total cross section $\sigma_{t,1}$, centered inside of a hemisphere with total cross section $\sigma_{t,2}$. The half-sphere has a 10 cm radius and the box is $10\sqrt{2}$ cm on a side and 5 cm tall. The mesh is illustrated in Fig. 6. The bottom of the entire hemisphere has a reflective boundary condition, the remainder of the exterior faces being vacuum. An isotropic unit source is distributed throughout the box. The scattering ratio is $c = 0.9999$.

Using AttilaV2 on a serial SGI Origin 2000 processor, we measured the number of iterations and number

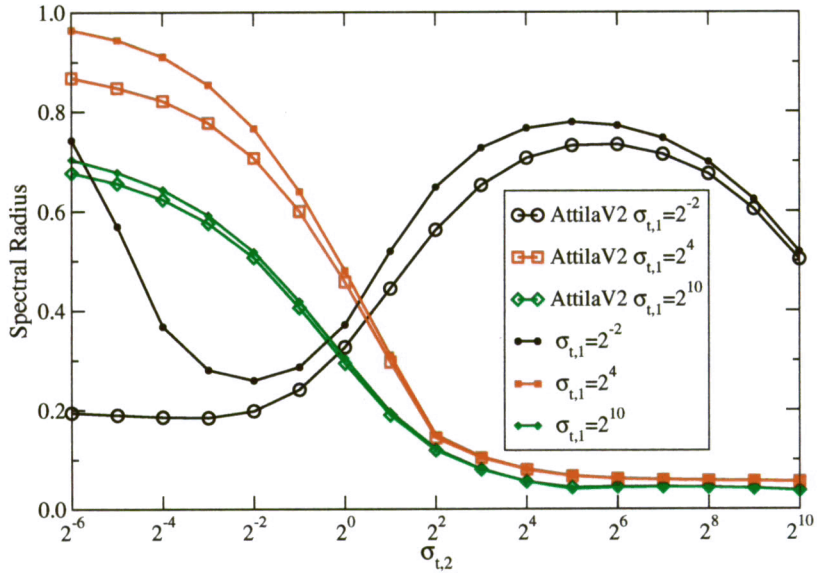

Figure 5. The spectral radius for FCDSA mwith $c = 0.999$ measured with the AttilaV2 code and compared to selected Fourier analysis results from the previous section.

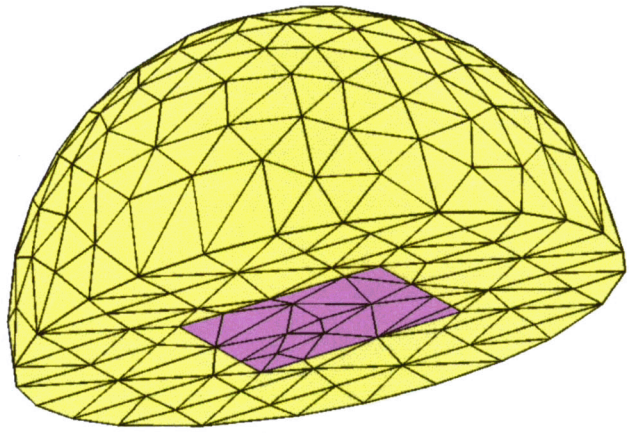

Figure 6. Mesh for a realistic heterogeneous problem consisting of two different materials as indicated by the shading in the figure. The bottom face is reflective and the box contains an isotropic distributed source of unit strength.

of floating point operations (FLOP) for convergence to a relative residual of 10^{-6} for this problem. A fixed stopping criteria of 10^{-7} was used for the inner DSA iterations. The measurements are shown in Tables I and II. The results are revealing. Firstly, note the upper right and lower left parts of both tables. These correspond to problems with regions containing both optically thin and thick regions, confirming that DSA loses its effectiveness in the presence of material discontinuities in realistic calculations. The iteration counts indicate the same kind of dependence, indicating a rise in the spectral radius for problems with material discontinuities. Secondly, the iteration counts show that when both regions are optically thick, the S-WLA method is not very effective while the FCDSA method is extremely effective. These observations are in agreement with the Fourier analysis predictions. Finally, despite the fact that FCDSA reduces the spectral radius and hence the number of iterations, the FLOP counts clearly indicate the high costs associated with solving the fully consistent diffusion equations, especially when the cells are very optically thin. On the other hand, even though the S-WLA method is less effective than FCDSA, illustrated by the iteration counts, the work per iteration can be much less, except when both materials are optically thick (the lower right part of the tables). The results of this section have shown that DSA will lose its effectiveness in the presence of material discontinuties, independent of the material configuration. Therefore, DSA can not be relied on to produce efficient solutions in general implementations.

5 FOURIER ANALYSIS IN THE ANALYTICAL LIMIT

With the results presented in Section 4 and the results in [8] and [9], the loss of DSA effectiveness for diffusive problems in the presence of material discontinuities has been established in both two and three dimensions with very different types of spatial discretizations. It is now clear that this effect appears is independent of the spatial discretization as well as the particular geometric configuration (the way the different materials are physically arranged).

The logical conclusion is that this is an analytical property of the DSA method in this situation and does not depend on the fact that we are working with spatially discretized equations. One way to confirm this is to investigate the DSA equations in the limit of the cell optical thickness approaching zero. Given a consistent spatial discretization – in the sense that a numerical approximation to the equation faithfully represents the continuous, analytical equation in the limit of a small discretization parameter – then examining the Fourier analysis in this limit will confirm this conclusion.

In this case, we set the width of the basic element (Fig. 1) to be $\Delta_x = \Delta_y = \Delta_z = 10^{-4}$. Then, we fix $\sigma_{t,1} = 10^{-4}$ while varying $\sigma_{t,2} = 2^{-n}\sigma_{t,1}$ over $n = 0, \ldots, 16$, a range of about 5 orders of magnitude. Both regions have the same scattering ratio c. The results are shown in Fig .7. Again, the results were repeated on a 24-tetrahedra basic element with differences only appearing in the fourth digit. We can see that by increasing the discontinuity in material in the direction of optical thin-ness, the loss in effectiveness increases with the size of the discontinuity.

An interesting question is what happens when the thin material not only has a small total cross section but is also not a diffusive material. This could be answered by setting the scattering ratio to a small value in the region where $\sigma_{t,2}$ is varied. These results are shown in Fig. 8 for a fixed scattering ratio of $c = 0.01$ in that region. When the problem is homogeneous, the spectral radius starts out smaller than when c is constant, but quickly rises back to the same levels as before. We also observed that making one of the materials non-diffusive in the numerical experiments did not change the results significantly.

$\sigma_{t,1}$	$\sigma_{t,2}$										
	2^{-10}	2^{-8}	2^{-6}	2^{-4}	2^{-2}	2^{0}	2^{2}	2^{4}	2^{6}	2^{8}	2^{10}
2^{-10}	4	4	6	8	11	16	nc	nc	nc	nc	nc
2^{-8}	5	5	6	8	11	16	22	26	29	28	22
2^{-6}	6	6	6	8	11	16	21	25	28	27	21
2^{-4}	9	9	9	9	10	14	18	22	24	24	19
2^{-2}	13	13	13	12	10	10	13	15	17	17	14
2^{0}	17	17	16	15	11	8	7	9	10	10	9
2^{2}	17	17	17	15	12	8	5	5	6	6	6
2^{4}	15	15	15	14	12	8	5	4	4	4	4
2^{6}	14	14	14	14	12	8	5	4	4	4	4
2^{8}	15	14	14	14	12	9	6	4	4	4	4
2^{10}	14	14	14	14	12	9	6	4	4	4	4

(a) Number of iterations

$\sigma_{t,1}$	$\sigma_{t,2}$										
	2^{-10}	2^{-8}	2^{-6}	2^{-4}	2^{-2}	2^{0}	2^{2}	2^{4}	2^{6}	2^{8}	2^{10}
2^{-10}	49.9	61.2	139	149	170	222	nc	nc	nc	nc	nc
2^{-8}	57.2	12.6	10.2	11.9	15.7	24.0	42.2	79.9	66.9	48.4	29.0
2^{-6}	127	12.0	4.69	5.56	7.16	10.4	13.2	15.5	17.4	16.2	12.9
2^{-4}	84.4	16.2	6.63	3.41	3.29	4.57	5.74	7.13	7.76	7.71	5.94
2^{-2}	118	23.0	9.27	4.27	2.05	1.84	2.41	3.04	3.75	3.66	2.60
2^{0}	175	24.5	10.9	5.11	2.11	1.15	1.02	1.49	1.87	1.82	1.38
2^{2}	146	24.5	11.5	5.07	2.25	1.15	0.68	0.77	1.00	0.96	0.87
2^{4}	118	21.7	10.2	4.77	2.33	1.28	0.74	0.59	0.61	0.59	0.57
2^{6}	109	20.0	9.46	4.79	2.58	1.41	0.78	0.60	0.58	0.58	0.56
2^{8}	145	18.7	9.38	4.73	2.54	1.49	0.92	0.58	0.57	0.55	0.53
2^{10}	187	19.3	9.25	4.60	2.22	1.32	0.81	0.55	0.55	0.52	0.47

(b) FLOP counts (billions)

Table I. Computational results with FCDSA for a realistic hetereogeneous problem containing two materials whose total cross sections are $\sigma_{t,1}$ and $\sigma_{t,2}$ (cm^{-1}). An entry "nc" indicates that the problem did not converge in 4 CPU hours.

$\sigma_{t,1}$	$\sigma_{t,2}$										
	2^{-10}	2^{-8}	2–6	2^{-4}	2^{-2}	2^{0}	2^{2}	2^{4}	2^{6}	2^{8}	2^{10}
2^{-10}	4	4	6	8	13	34	109	242	345	344	205
2^{-8}	5	5	6	8	13	33	103	222	316	317	190
2^{-6}	6	6	6	8	13	30	86	174	254	259	164
2^{-4}	9	9	9	9	12	24	60	117	173	184	127
2^{-2}	14	14	14	13	11	18	40	77	114	125	97
2^{0}	32	31	30	25	18	21	40	72	103	115	96
2^{2}	89	87	80	64	44	41	60	87	128	143	124
2^{4}	182	177	160	126	84	73	98	123	163	184	177
2^{6}	244	235	211	164	109	90	123	150	182	206	208
2^{8}	272	261	229	176	118	91	119	147	188	208	204
2^{10}	186	178	160	131	88	72	94	132	185	198	160

(a) Number of iterations

$\sigma_{t,1}$	$\sigma_{t,2}$										
	2^{-10}	2^{-8}	2^{-6}	2^{-4}	2^{-2}	2^{0}	2^{2}	2^{4}	2^{6}	2^{8}	2^{10}
2^{-10}	0.10	0.10	0.14	0.17	0.27	0.69	2.18	4.82	6.87	6.84	4.08
2^{-8}	0.12	0.12	0.14	0.17	0.27	0.67	2.06	4.42	6.29	6.30	3.78
2^{-6}	0.14	0.14	0.14	0.17	0.27	0.61	1.72	3.46	5.05	5.15	3.26
2^{-4}	0.20	0.20	0.19	0.19	0.25	0.49	1.20	2.33	3.44	3.66	2.52
2^{-2}	0.30	0.30	0.30	0.27	0.23	0.37	0.81	1.54	2.27	2.48	1.93
2^{0}	0.66	0.64	0.62	0.51	0.37	0.43	0.8	1.44	2.05	2.28	1.90
2^{2}	1.80	1.76	1.61	1.29	0.89	0.82	1.20	1.73	2.54	2.82	2.44
2^{4}	3.67	3.56	3.21	2.53	1.68	1.45	1.95	2.44	3.21	3.62	3.47
2^{6}	4.91	4.72	4.23	3.28	2.17	1.79	2.44	2.96	3.57	4.03	4.07
2^{8}	5.48	5.25	4.59	3.52	2.35	1.81	2.35	2.90	3.68	4.06	3.98
2^{10}	3.75	3.58	3.21	2.62	1.75	1.43	1.86	2.60	3.62	3.86	3.12

(b) FLOP counts (billions)

Table II. Computational results with the S-WLA scheme for a realistic hetereogeneous problem containing two materials whose total cross sections are $\sigma_{t,1}$ and $\sigma_{t,2}$ (cm^{-1}). An entry "nc" indicates that the problem did not converge in 4 CPU hours.

These two figures confirm the fact this is an analytical property of the DSA method.

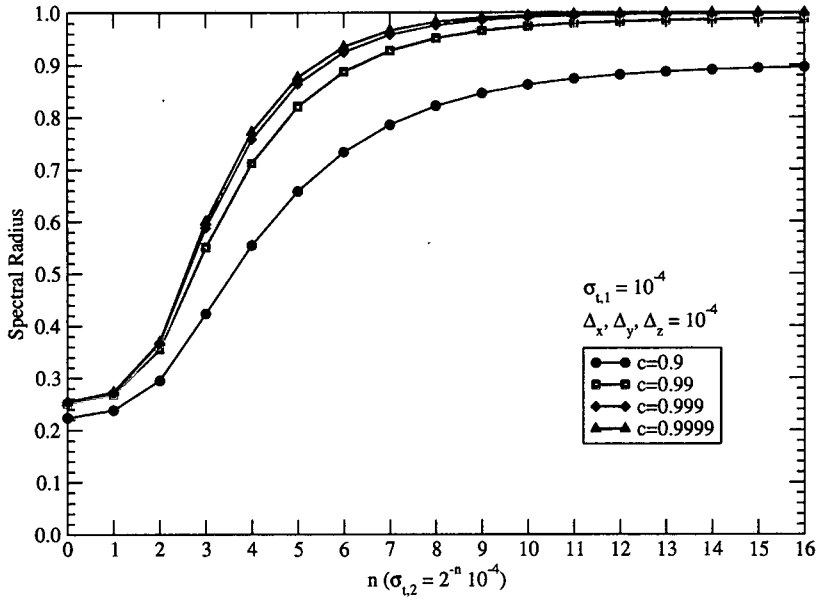

Figure 7. Fourier analysis in the optically thin limit for a fully consistent DSA method. The scattering ratio, c, is the same in both materials.

6 CONCLUSIONS

We conclude that in a multidimensional problem with a scattering ratio approaching unity the effectiveness of all DSA methods can degrade in the presence of material discontinuities because it is an property of the analytical DSA method. This does not depend on what the particular geometric configuration might be or whether a DSA method is is consistently discretized or not. Inconsistency probably just makes the situation worse; How much will depend on the particular method.

So we are left in the undesirable situation where acceleration of transport source iterations with DSA cannot be relied upon to produce efficient solutions in all circumstances. This is particularly true in the diffusive problems where DSA is most needed. However, in another paper that we plan to present at this conference, we will show that replacing source iteration with a more powerful iterative method enables us to use the efficient, partially consistent S-WLA DSA scheme to compute transport efficiently in heterogeneous and diffusive problems.

Acknowledgments

This work was performed under the auspices of the U.S. Department of Energy at the Los Alamos National Laboratory. The authors thank Yousry Azmy and Ed Larsen for their helpful and insightful comments on this topic.

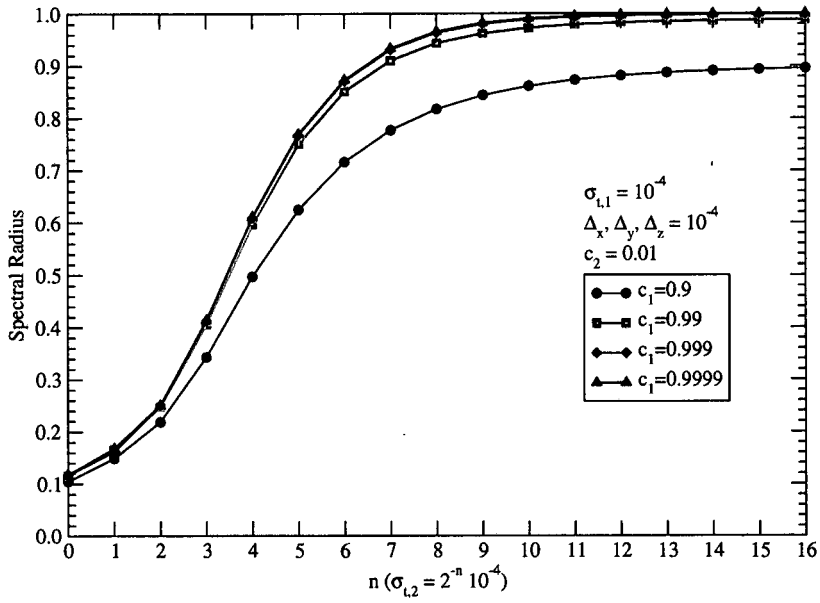

Figure 8. Fourier analysis in the optically thin limit for a fully consistent DSA method. Note that the scattering ratio in the thin region is fixed at $c_2 = 0.01$.

REFERENCES

[1] R. E. Alcouffe, "Diffusion Synthetic Acceleration Methods for Diamond–Differenced Discrete–Ordinates Equations," *Nucl. Sci. and Engr.*, **64**, pp. 344–355 (1977).

[2] E. W. Larsen, "Unconditionally Stable Diffusion–Synthetic Acceleration Methods for Slab Geometry Discrete Ordinates Equations. Part I: Theory," *Nucl. Sci. and Engr.*, **82**, pp. 47–63 (1982).

[3] D. R. McCoy and E. W. Larsen, "Unconditionally Stable Diffusion–Synthetic Acceleration Methods for Slab Geometry Discrete Ordinates Equations. Part II: Numerical Results," *Nucl. Sci. and Engr.*, **82**, pp. 64–70 (1982).

[4] M. L. Adams and T. A. Wareing, "Diffusion-Synthetic Acceleration Given Anisotropic Scattering, General Quadratures, and Multidimensions," *Trans. of the Am. Nucl. Soc.*, **68**, pp. 203–204 (1993).

[5] J. S. Warsa, T. A. Wareing, and J. E. Morel, "Fully Consistent Diffusion Synthetic Acceleration of Linear Discontinuous Transport Discretizations on Three–Dimensional Unstructured Meshes," *Nuclear Science and Engineering*, **141**, pp. 236–251 (2002).

[6] M. L. Adams and W. R. Martin, "Diffusion Synthetic Acceleration of Discontinuous Finite Element Transport Iterations," *Nucl. Sci. and Engr.*, **111**, pp. 145–167 (1992).

[7] T. A. Wareing, "New Diffusion–Synthetic Accelerations Methods for the S_N Equations with Corner Balance Spatial Differencing," in **Joint International Conference on Mathematical Methods and Supercomputing in Nuclear Applications**, 19–23 April, Vol. 2, Karlsruhe, Germany, p. 500 (1993).

[8] Y. Azmy, "Impossibility of Unconditional Stability and Robustness of Diffusive Accleration Schemes," in **1998 American Nuclear Society Radiation Protection and Shielding Division Topical Meeting**, 19–23 Apr, Vol. 1, Nashville, TN, p. 480 (1998).

[9] Y. Azmy, T. Wareing, and J. Morel, "Effect of Material Heterogeneity on the Performance of DSA for Even–Parity S_N Methods," in **International Conference on Mathematics and Computation, Reactor Physics, and Environmental Analysis in Nuclear Applications**, 27–30 Sep, Vol. 1, Madrid, Spain, pp. 55–63 (1999).

[10] T. A. Wareing, J. M. McGhee, J. E. Morel, and S. D. Pautz, "Discontinuous Finite Element S_n Methods on Three–Dimensional Unstructured Grids," *Nuclear Science and Engineering*, **138**, pp. 1–13 (2001).

[11] E. E. Lewis and W. F. Miller, **Computational Methods of Neutron Transport**. Wiley & Sons: New York (1984).

[12] M. L. Adams, "Discontinuous Finite Element Methods in Thick Diffusive Problems," *Nucl. Sci. and Engr.*, **137**, pp. 298–333 (2001).

[13] H. J. Kopp, "Synthetic Method Solution of the Transport Equation," *Nucl. Sci. and Engr.*, **17**, p. 65 (1963).

[14] E. M. Gelbard and L. A. Hageman, "The Synthetic Method as Applied to the S_n Equations," *Nucl. Sci. and Engr.*, **37**, pp. 288–298 (1969).

[15] R. E. Alcouffe, "Diffusion Synthetic Acceleration Methods for the Diamond-Differenced Discrete-Ordinate Equations," *Nuclear Science and Engineering*, **64**, pp. 344–355 (1977).

[16] E. W. Larsen, J. E. Morel, and W. F. Miller, Jr., "Asymptotic Solutions of Numerical Transport Problems in Optically Thick, Diffusive Regimes I," *J. Comp. Phys.*, **69**, pp. 283–324 (1987).

[17] E. W. Larsen and J. E. Morel, "Asymptotic Solutions of Numerical Transport Problems in Optically Thick, Diffusive Regimes II," *J. Comp. Phys.*, **83**, pp. 212–236 (1989).